ALKALI SILICA REACTION IN CONCRETE: KINETIC MODELING THE START OF THE EXPANSION. PART 1- MODEL ASSUMPTIONS, STRUCTURE AND DATA FITTING

Luís Mayor Gonzalez[1*], António Santos Silva[2], Dora Soares[2], Said Jalali [1]

[1] Department of Civil Engineering, University of Minho, Guimarães, Portugal

[2] Materials Department, National Laboratory for Civil Engineering (LNEC), Lisboa, Portugal

Abstract

Service life, in alkali-silica reaction (ASR) affected concretes, is reached when expansions no longer allow normal use of a structure. ASR expansions are detected after a long period, accelerating after that, similarly to reactions with induction period in Chemical Kinetics.

This study considers service life as induction time, and uses kinetic methods in its estimate. The classical Unreacted Shrinking Core (USC) model with diffusion control and induction time was selected, among other models. Both plane and spherical interfaces were considered adapting their models to expansion input. ASTM C 1260 test conditions and setup were selected, its near constant alkalinity being closer to initial conditions in concrete. Mortar bars with a reactive Tagus river aggregate were tested at temperatures of 80, 70, 60, 50 and 37ºC. Plane and spherical expansion models were fitted to isothermal curves, depicting their kinetic parameters in Arrhenius plots that suggest the spherical model as better.

Keywords: Alkali-Silica Reaction, prevision, model, induction time

1 INTRODUCTION

Service life is commonly used as a durability indicator. In the case of a concrete affected by the Alkali-Silica Reaction (ASR), service life is the age at which expansions no longer allow the normal utilization of a structure. The relevance of such expansion depends on the kind of structure, significant values being reported from near 0.02% (for dams[1] [Scrivener 2010]) to about 0.2% (for a pier [2] [Myaga and Miura, 2006]). A general default value of 0.04% is considered, as widely accepted, for microcracking to be seen (e.g., Grattan-Bellew 1983)[3].

In the case of highly reactive aggregates, the ASR expansion is generally slow at beginning, but accelerates quickly after a certain time. This overall behavior is similar to a reaction with induction time, and the approach followed in this work is to assume service life as the induction time estimated by the methods used in chemical kinetics of reactions. Under the physical model perspective, induction time was interpreted by some authors as the time needed for the alkali gel to form, expand and fill in the space between the aggregates external surface and the pores in the cementitious paste [Diamond 1981, Ichikawa 2007] [4, 5].

As a global method, this approach allows using expansion models without need of detailing the nature and influence of all underlying processes (only controlling process are relevant), provided that the curve of conversion is sigmoid shaped, even if there is no induction, *strictu senso*. Gonzalez et al 2001 listed different physical and chemical processes leading to this same curve shape [6]. The underlying phenomena affect, however, other aspects of the reaction, like products morphology or development of porosity, stoichiometry

* Correspondence to: lmgonzalez@mail.telepac.pt

and parallel reactions. It is a useful approach, but subject to an evaluation of the agreement between model and reality. A check of microstructure changes may be particularly relevant whenever possible. To model induction time, it is convenient for conditions to be as steady as possible, to isolate the effect of the main known factors, alkalinity, humidity and temperature.

As a wide knowledge on ASR is provided by expansion tests in different test conditions, these test conditions were considered to define the more convenient set up of the experiments to carry out. Among the main expansion tests, the ASTM C 1260 mortar-bar test, is the only one that allows to consider a comparatively steady reaction environment regarding alkalinity, humidity and temperature, condition required to assign values to these main factors, even if it departs from concrete conditions in field, as seen below, and has precision limitations due to the dependence on reaction and reading temperatures. The other expansion tests available run under saturating conditions; so, the alkalinity decreases due to leaching and to the ASR itself (in the former test these variations are compensated by the immersion fluid).

It must be referred to that the conditions used in ASTM C 1260 test are designed for alkali reactivity determination; they are quite different from conditions in concrete under normal use, and so they are not appropriate to simulate the expansion during the entire concrete life, beyond the period in which expansion is very small. The method is thus selected just to model induction time. The models traditionally used to predict quantitatively concrete expansion are validated for normal concrete conditions, (e.g., the models referred to in the revisions by Moranville-Regourd 1997 [7] and Poyet 2003 [8]), and may not be adequate for the conditions now selected. In some of them, the alkalinity decrease has a relevant role on reaction slowing and halt, and thus may not be appropriate as they are based (or consider) the effect of alkalis and hydroxyl consumption.

Data from ASTM C 1260 test [9] were modeled using topochemical, diffusion controlled, and nucleation and growth models. A diffusion controlled model, with a plane interface, was used by Furusawa et al. 1994 [10] using data from the ASTM C 289 test [11], in conditions of excess alkalinity similar as those of ASTM C 1260 (though focused on silica dissolution rather than strain development, and during a shorter period). The nucleation and growth model was referred to by Pade and Struble 2000 [12] and by Johnston and Fournier 2000 [13]. These last authors used the test ASTM C 1260 to model expansion and characterize the reactivity through the kinetic parameter associated to growth rate. The topochemical model, diffusion controlled, is also consistent with the remarks of many authors on the importance of diffusion, considered by some even as controlling step. The induction time may be inserted in this model as an additive constant (Murayama et al. 1994) [14], assuming a null strain for ages lower than induction time. Induction time is an abstract notion and its formulation depends on the model considered. For a better understanding, the models are briefly sketched.

The more general topochemical model is the model USC **(unreacted shrinking core)**, applied in its original form [Levenspiel 1972] [15] to non catalytic heterogeneous reactions with non porous solid reagent, assuming that the reaction occurs by removal or incorporation of part of fluid reagent, in the interface between solid reagent and solid product. The conversion of solid reagent into product, occurring uniformly where the reaction takes place, displaces, as a whole, the interface to inside of the reagent phase, the reaction progressing along a direction normal to the interface. This limit situation is ideal; usually the reaction takes place in a more diffuse way, and would be better described by a reaction front with a certain "depth", along which unreacted to completely reacted material is found. The overall description of reaction progress is however similar or equivalent (an early work found a proportional relation to exist between areas of sharp and diffused fronts, globalised in the kinetic constant). The physical progression of the reaction front, i.e., of the interface, measures thus the extent of global transformation, and may be expressed by the amount of remaining solid reagent (ahead the interface) or the amount of product formed (behind the interface). Often,

full conversion is not achieved locally and the front progress leaves behind a heterogeneous mix of reacted and unreacted product keeping a certain uniformity regarding its components proportion and grain size, as well as the microstructure of pores and fissures, and is called "ash", when such designation is not confusing. In its original form, the model considers 3 potentially controlling stages, that may appear as single control (of each stage), and as mixed control of 2 or even 3 stages. The 3 control stages considered are surface reaction, diffusion through the products layer ("ash"), and the diffusion of fluid reagent through the boundary layer external to the particle. The complete mechanism considers two more stages of diffusion of products through the fluid phase up to the bulk fluid, with similar formulation to the diffusion of fluid reagent (the distinction between these 2 stages and the former ones is not easy, and is seldom done). The driving force of the reaction is the difference of reagent concentration between bulk fluid and the equilibrium concentration at the solid surface; it is broken down in parcels for those 3 stages, considering intermediate concentrations at the external surfaces of the initial particle and at the unreacted core. In this model a constant reaction rate per unit interface area is assumed; in diffusional stages, the processes follow the laws of diffusion, with simplifying assumptions as the existence of a pseudo-stationary state

The model is easy to develop in the case of only one reaction, assuming constant the concentration of the bulk fluid, as it may be reasonable to accept in tests with immersed bars such as ASTM C 1260, and in certain conditions lead to relatively simple equations [Levenspiel 1972], for interfaces with plane, long cylinder and spherical shape. Usui et al.1994 and Murayama et al 1994 [14, 16] present more complex models for several sequential or intermediate reactions, (in most cases only one of these is controlling and needs to be considered for kinetic modeling). This model found a wide application even outside its original scope of validity, being reported namely in porous materials in certain conditions, in reversible reactions and for fluid reagent deprived conditions. This lead, in part, to development of new models derived or based on this model, such as the crackling core model, the grain or structural model (applied to porous materials), and Sohn's model, this one associating to the usual controlling stages a nucleation and growth stage.

For single ash diffusion control the equation is [Levenspiel 1972]:

For plane interface $$t = \rho_B/(6bD_eC_A)\ (\Delta x)^2 \quad (1)$$

For spherical interface $$t = \rho_B R^2/(6bD_eC_A)\ (\Delta r/R)^2\ [1- 3(r/R)^2+2(r/R)^3)] \quad (2)$$

where ρ_B is the molar density of the solid reagent, b is a stoichiometric coefficient, D_e is the effective diffusion coefficient inside solid product (ash), C_A is the concentration of concentration of fluid reagent in the fluid phase, Δx is the thickness of the solid product layer, R is the radius of the aggregate particle, when assumed spherical, r is the radius of the unaffected grain, and $\Delta r = R - r$ is the reaction front progress, close the thickness of the solid product shell (equals it when there is no expansion or retraction).

No induction time is considered in this original model. When the conversion curve is sigmoidal, induction time may be added as a constant term [14]. The model thus defined contains a discontinuity due to the sudden change of the derivative value, and naturally is not appropriate to represent what happens, in a continuous way, within the induction period. Its application is valid [Gonzalez et al. 2001], when this period is not relevant beyond simply adjusting the start of the subsequent stages.

For plane interface $$t = tind + \rho_B/(6bD_eC_A)\ (\Delta x)^2 \quad (3)$$

For spherical interface $$t = tind + \rho_B R^2/(6bD_eC_A)\ (\Delta r/R)^2\ [1- 3(r/R)^2+2(r/R)^3)] \quad (4)$$

The **nucleation and growth model**, or Avrami's (the designation of Erofeev´s, or Kolmogorov´s, also often appears, sometimes with variations in assumptions and meaning of the parameters) assumes that the transformation of solid reagent in product occurs through a continuous formation of nuclei, with even probability everywhere in the space still occupied by the reagent, followed locally and immediately by the growth around each nucleus at the reagent-product interface, in several directions, at a constant rate; the growth stops when another interface is found, i.e., all reagent is locally consumed. Thus, nucleation precedes growth only locally, for each nucleus, but may coexist in different nuclei. The correspondent equation is:

$$\alpha = 1 + \alpha_o - e^{-k(t-t_o)^M} \quad (5)$$

where α is the conversion (between 0 e 1), α_o is the initial expansion at t_o, 4th day of cure, k is a kinetic constant and M is the exponent.

In this model, with shape intrinsically sigmoidal, there is no parameter that may be called induction time (in the case of a reaction with a real induction, it would occur *before* nucleation). However, we may physically associate it with the microstructure change caused by the initial formation of nuclei, and related acceleration, though the model itself considers such nuclei formation as well as their growth not confined to an initial stage, but extended permanently, lasting until the reaction is complete.

In terms of conversion curve, this idea of "induction" allocated to an initial period with low reaction rate, is accepted and currently applied, e.g., over the conversion curve plot, taking as "induction time" the abscissa of the point where the time axis is crossed by the tangent to the conversion curve, where this is as linear as possible: in the USC model with induction time, this leads exactly to the additive term considered; in the nucleation and growth model it leads to an "equivalent induction time". Gonzalez et al. 2001[6] used the equation of this last model (being a continuous function) to evaluate this parameter, objective and analytically, after the inflexion point position (where second derivative is null), the tangent value (by the first derivative) at that point and thus, by elementary analytical geometry, of the abscissa of the point where the tangent line cuts the time axis. However, although allowing a good fit to data at higher temperatures, this model was discarded because the "induction time" estimate by the Avrami model present difficulties at lower temperatures, for which the curvature is less pronounced. Johnston and Fournier 2000 refer a dependence, though ill-defined, between the exponent of the model and the alkalinity. This dependence render difficult the application of a model developed from an aggregate tests with a cement type, to concretes with same aggregates but different alkali contents (by change of cement quality, or external additions).

The present work adapts the equations of the USC model with ash diffusion control, for plane and spherical interfaces, to the actual case, considering expansion proportional to reaction extent, allowing to use directly expansion data in percentage or fraction. A series of data is then used to determine the kinetic parameters by least squares fitting, as well as the dependence of the found parameters on the temperature factor. This model of expansion kinetics is complemented with models taken from the literature, for the effect of humidity and alkalinity, in function of the quality of cement in use.

2 EXPERIMENTAL

2.1 Observation by optical and scanning electron microscopy

In the case of ASR, some authors (Helmut et al. 1993 [17], Scrivener and Monteiro 1994 [18], Kawamura 1997 [19]) refer the existence of an external layer altered by cracking, the presence of alkali and calcium ions and a variation of micro-hardness. A reaction rim is referred in some cases [Ichikawa 2007 [5] , Rivard 2002 [20], Moranville-Regourd 1989 [21]]. The existence of an unreacted core beyond a certain alteration depth was underlined in these works. With the exception of the reaction rim, they don´t mention though the existence of a clearly defined interface (a reference [18] mentions that no such interface or limit

could be found, despite detecting a concentration variation), and consequently a product shell, what doesn't alter the essential assumptions of the procedure carried out.

The aggregate used, being a mix, was difficult to check for microstructure variations. However it is known that a major component is reactive silica from quartzites or strained quartz grains. Observations were carried on granite aggregate, around an attacked quartz grain was identified, assumed to be similar to at least some of sands components from a river crossing a large granitic area.

Observations were carried out by optical microscope, for resin penetration in fissures and, in nearly crossed polars, for the sub grain microstructure, to check eventual relation between fissuration and crystallite boundaries, and, at the scanning electron microscope, of general microstructure, including fissures and element distribution, as element maps and profiles.

2.2 Expansion tests

Experimental data were obtained from mortar bars, prepared with a alluvial reactive siliceous aggregate from Tagus river in Portugal, immersed in 1M NaOH, according to the set up of ASTM C 1260 test, at temperatures of 80, 70, 60, 50 and 37 ºC, to model expansion at constant alkalinity, as function of aggregate reactivity and temperature.

3. RESULTS PROCESSING AND DISCUSSION

Observation

By optical observation, Figures 1 and 2 show a monocrystalline grain of undulatory, strained quartz at nearly crossed polars (Figure 1) and inside it, resin penetration in peripheral, intra-crystallite micro-cracking (Figure 2). A general pattern of tangential and radial cracks, is denser in zones of higher curvature, and leaves a less affected core, and preferential peripheral expansion and reaction front progress inwards may be inferred. Note the radial crack in the lower right corner of the grain (cf. Pade and Struble 2000, Golterman 1994, 1995) [12, 22, 23]. Golterman [22, 23] analyzed the relation between local peripheral expansions and tensions field inside particles, and the potential cracking pattern. In case of polycrystalline grains, the reaction may be less uniform, concentrating on the inter-crystallite siliceous cement in quartzites, or grains of unstable nature, like cristobalite or tridymite.

A possible "ash" shell formed after the reaction inwards progress is suggested by Figure 3, of a SEM oxygen map of a strained quartz grain in a concrete thin lamella. Local formation of amorphized silica with considerable expansion is the first step of silica attack (opening siloxane bridges) as referred to, i.a., by Bulteel and Garcia Diaz [24, 25] :

$$2\ SiO_2 + OH^- + Na^+ \Rightarrow H\ Si_2O_5^- + Na^+$$

These authors quantified the expansion due to the transition from Q^4 to Q^3 in the protonised form of this material. This transition is associated with an increase of the ratio O/Si, due to the reaction itself (from 2 to 2.5) and subsequent cations adsorption and hydration (the presence of solvated ions and water molecules may rise the ratio), and is followed by a silica dissolution step; the value of 2.5 is found in solid products identified by some authors with the reaction (amorphized silica, kanemite, oekonite and other Q3 silicates).

Radial cracks, along which oxygen enrichment is higher, are also evidenced in Figure 4 as a cracking pattern denser in the periphery, showing alkali-calcic gel penetration in the corresponding Calcium map of the same field, cropped and enlarged to enhance details. The relation shown between an oxygenated, expansion-reacted shell and a peripheral crack pattern suggested in figures 3 and 4, although, was not checked in other observations. Both features, O/Si and peripheral microcracking, may be interrelated, denoting an expansive degrading reaction progressing inwards, leaving an outer, reaction affected shell.

Expansion tests results and modelling

Expansion data below 0.25% for isothermal curves at 80, 70, 60 and 50ºC are plotted in Figure 6, as well as data for the longer 37.2 ºC run. The data, particularly for the last curve is too numerous to allow tabling.

The topochemical model by ash diffusion control was adapted to expansion data, considering that the expansion is the result from the (proportional) effect, at bar level, of the expansion of aggregate particles with a uniform size, R, constituting the aggregate skeleton of the concrete. For this, equations (3) and (4) were re-formulated to made explicit the dependence on expansion, rather than reaction extent, by making $\Delta r = R - r = k.\varepsilon$, what corresponds to:

$$t - tind' = \rho_B R^2/(2bD_eC_A)\ (\Delta r/R)^2\ [1-(2/3)(\Delta r/R)] \quad (6)$$

plane interface $$t = tind + C\ (\Delta x)^2 = tind + C\ (k.\varepsilon)^2, \quad (7)$$

spherical interface $$t = tind' + C'\ (\Delta r/R)^2\ (1-2/3\ \Delta r/R) = tind' + C'\ (k.\varepsilon)^2\ (1-2/3\ k.\varepsilon) \quad (8)$$

These equations were fitted to experimental data, for determination of kinetic parameters using only the curves at 50 to 80ºC. Data with expansions below 0.04 – 0.06% were not included in this fitting of isothermal data. The kinetic parameters thus extracted are then represented as Arrhenius plots, as shown in figure 5, high correlation coefficients having been obtained. For the plane model, k is incorporated in the constant C. For the spherical model, least squares were applied numerically, using the SOLVER command of EXCEL to determine k, as constant for all temperatures. The linear representation allows an easy modeling by regression of the dependence of said parameters on the temperature.

Figure 5 shows that for induction time, the correlation coefficient is higher in the case of spherical interface; this should be expected as its equation is more general. Applying the equations obtained for C, tind, C' and tind', the models may express estimated times as function of expansions and temperature, as shown only for the spherical case below in Equation (9):

$$t = \exp(-22.313).\exp(-8262.6/RT) + [\exp(-17.891).\exp(7871.1/RT)].(k.\varepsilon)^2 . (1-2/3\ k.\varepsilon) \quad (9)$$

The estimates are represented in Figure 6, along with the corresponding experimental data. For the upper expansions there is a general good agreement, except for deviations in curves at 50 and 70 ºC, where all deviations, although small, are systematically to one side, and clearly better for the spherical interface case. Figure 6 evidences further, for the prediction of induction time at 37.2ºC, a better fitting of the model with spherical interface in comparison with plane interface. At this temperature, however, the higher expansions curve depart significantly from data, with even a different pattern.

The correlations thus obtained allow to estimate at each temperature, the induction time and the resulting curve of strain against time, and the other mentioned factors, only for laboratory conditions. But only the induction time, the first parcel in equation 9, estimates can be considered as acceptable from the present work.

4. Conclusions

The shape similarity between usual expansion curves obtained for alkali testing of aggregates, and conversion curves of reaction with induction time, lead to the present approach of estimating the service life by the induction time determined by chemical kinetics methods. The model selected to fit experimental data

was the classical unreacted shrinking core model. The induction time was formulated according the model selected, as an additive constant depending on the temperature. Two interface shapes were analyzed, plane and spherical, fitted and compared. The spherical interface model presented a better fit, in terms of the induction time correlation, which was confirmed by an independent test at 37.2ºC.

Figure 6 shows the large influence of the temperature factor on the results, by a variation of ±-2 around 37.2ºC. This strong influence, *ca* 15 % in time for a 2 degrees variation, suggests the need of an independent reading of the temperatures in use, with precision of 1/10th ºC. Temperature off setting within the test allowance may also be a cause for the systematic deviations found in 50 and 70 º C .This should not be confused with the always relevant need of a special attention to the reading conditions of expansions in which the bar is subject to a temperature variation.

A more detailed discussion of the data and estimated curves is presented in Part II of this paper

ACKOWLEDGEMENTS

The authors thank the financial support provided by **Fundação para a Ciência e Tecnologia (FCT)**, through the project EXREACT (PTDC/CTM/65243/2006).

REFERENCES

[1] Scrivener, K., Dunnant, C.," Modelling ASR with AMIE" in Research progress conference, RILEM 2010. Azores.

[2] Miyagawa, T., Seto, K., Sasaki, K., Mikata, Y., Kuzume, K., Minami, T., "Fracture of Reinforcing Steels in Concrete Structures Damaged by Alkali-Silica Reaction -Field Survey, Mechanism and Maintenance-", Journal of Advanced Concrete Technology, 4, 2006, 3, 339-355

[3] Grattan-Bellew, P.E., "Evaluation of Test Methods for Alkali-Aggregate Reactivity", Danish Concrete Association, 6th International Conference Alkalis in Concrete: Research and Practice, Technical University of Denmark, Copenhagen, June 1983, pp. 303-14.

[4] Diamond, S., R. Barneyback and L.J. Struble. *On the physics and chemistry of alkali–silica reactions*. in *5th International Conference on Alkali-Aggregate Reaction in Concrete*. 1981. Cape Town, South Africa

[5] Ichikawa, T., Miura, M., "Modified model of alkali-silica reaction", Cement and Concrete Research, Vol. 37, No. 9, September 2007, pp. 1291-1297

[6] Gonzalez, L.M., Nogueira, C.A., Romero, J.B., "Comparação de modelos cinéticos para reacções heterogéneas não catalíticas, considerando tempo de indução" ("Comparison of kinetic models for non catalytic heterogeneous reactions, considering induction time"), 8th International Chemical Engineering Conf., (Ed. F. Ramôa Ribeiro e J.J. Cruz Pinto), Aveiro, Setembro 2001, pp. 223-230.

[7] Moranville-Regourd, M., "Modelling of Expansion Induced by ASR–New Approaches", Cement and Concrete Composites, Vol. 19, 1997, pp. 415-425.

[8] Poyet, S., "Etude de la dégradation des ouvrages en béton atteints par la réaction alcali-silice: Approche expérimentale et modélisation numérique multi-échelles des dégradations dans un environnement hydro-chemo-mécanique variable", THÈSE grade de Docteur Génie Civil, l'Université de Marne-La-Vallée, Décembre 2003.

[9] ASTM C 1260, "Standard test method for potential alkali reactivity of aggregates (mortar-bar method)", ASTM International, West Conshohocken, United States, 2007.

[10] Furusawa, Y., Ohga, H., Uomoto, T., "An analytical study concerning prediction of concrete expansion due to alkali-silica reaction", In: Malhotra, Editor, 3rd Int. Conf. on Durability of Concrete, Nice, France, 1994, pp. 757–780 SP 145–40.

[11] ASTM C 289 Standard Test Method for Potential Alkali-Silica Reactivity of Aggregates (Chemical Method).

[12] Pade, C., Struble, L., "Kinetics and Microstructural Changes Associated with Mortar Expansion", Cement, Concrete and Aggregates, Vol. 22, No. 1, 2000

[13] Johnston, D., Fournier, B.A., "A Kinetic-Based Method for Interpreting accelerated mortar bar test (ASTM C 1260) data", Proc. 11th International Conf. on Alkali-Aggregate Reaction, Quebec, 2000, pp. 355- 364.

[14] Murayama, T., Usui, T., Naito, M., Ono, Y., "Kinetic Analysis on Gaseous Reduction Of Agglomerates, part 2 Rate Parameters Included in the Mathematical Models for Gaseous Reduction of Agglomerates", Tetsu-to-Hagané, 1994. 80(7), p. 493-500

15] Levenspiel, O., "Chemical Reaction Engineering", Wiley, 1972.

[16] Usui, T., Naito, M., Murayama, T., Morita, Z., "Kinetic Analysis on Gaseous Reduction of Agglomerates, Part 1 Reaction Models for Gaseous Reduction of Agglomerates", Tetsu-to-Hagané, Vol 80, (1994), 6, 431-439

[17] Helmuth, R., Stark, D., Diamond, S., Moranville-Regourd, M., "Alkali-Silica Reactivity: An Overview of Research", Monograph, SHRP-C-342, Strategic Highway Research Program National Research Council, Washington DC, 1993.

[18] Scrivener, K.L., Monteiro, P.J.M., "The Alkali-Silica Reaction in a Monolithic Opal", Journal of the American Ceramic Society, Vol. 77, No. 11, 1994, pp. 2849-2856

[19] Kawamura, M., Komatsu, S., "Behavior of Various Ions in Pore Solution in NaCl-bearing Mortar with and without Reactive Aggregate at Early Ages", Cement and Concrete Research, Vol. 27, No. 1, 1997, pp. 29-36.

[20] Rivard, P., Ollivier, J.-P. Ballivy, G., "Characterization of the ASR rim Application to the Potsdam sandstone", Cement and Concrete Research 32 (2002) 1259–1267.

[21] Moranville-Regourd, M., Products of Reaction and Petrographic Examination. in 8th International Conference On Alkali-Aggregate Reaction In Concrete. 1989,. Kyoto

[22] Goltermann, P., "Mechanical Predictions on Concrete Deterioration. Part 1: Eigenstresses in Concrete", ACI Materials Journal, Vol. 91, No. 6, 1994, pp. 543-550.

[23] Goltermann, P., "Mechanical Predictions of Concrete Deterioration; Part 2: Classification of Crack Patterns", ACI Materials Journal, Vol. 92, No.1, 1995, pp. 58-63.

[24] Bulteel, D., Garcia-Diaz E, Siwak, J M, Vernet, C, Zanni, H, "Alkali-aggregate reaction : A kinetic study", Conference Infrastructure regeneration and rehabilitation improving the quality of life through better construction : a vision for the next millennium 1999. Sheffield.

[25] Verstraete, J., Khouchaf, L., Bulteel, D. ,Garcia-Diaz, E., Flank, A. M, Tuilier, M. H., "Amorphisation mechanism of a flint aggregate during the alkali–silica reaction: X-ray diffraction and X-ray absorption XANES contributions", Cement and Concrete Research, Vol 34, Issue 4, 2004, 581-586

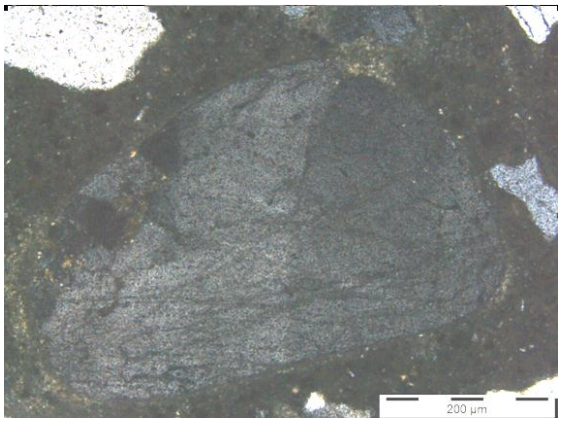

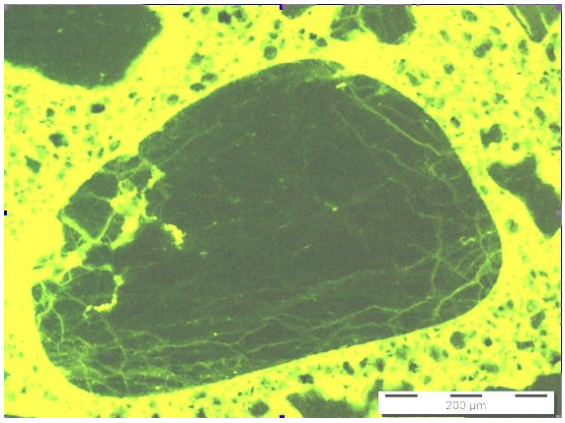

Figures 1 and 2: Optical microscope of a monocrystalline grain, nearly crossed polars (left, Figure 1) and a observation of resin penetration in cracks (see text) .

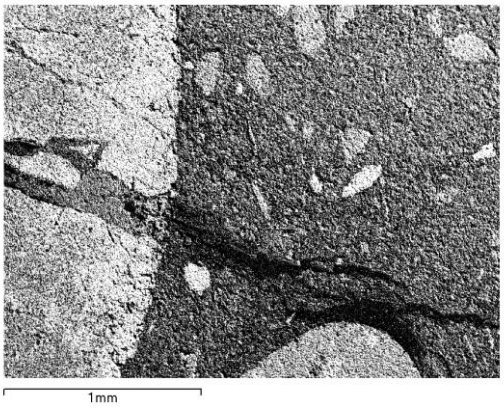

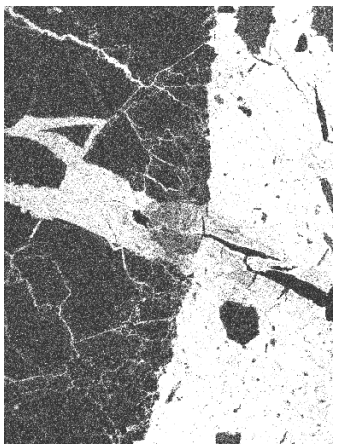

Figures 3 and 4: A strained quartz grain with preferential peripheral enrichment in oxygen mapped image (Figure 3) and enlarging the same field, a cracking pattern, denser in the periphery, in a calcium mapped image (Figure 4).

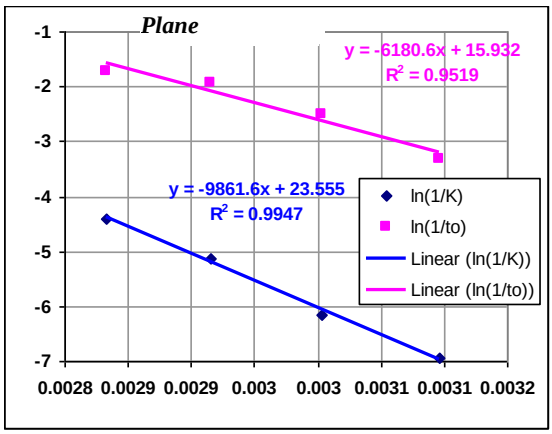

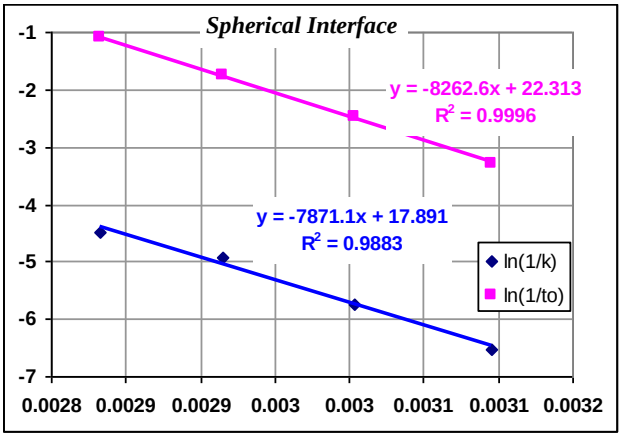

Figure 5 Arrhenius plots for "ash" diffusion models with plane and spherical interface; **k** represents, according to the model, **C** (plane interface) or **C'**(spherical interface); the upper curve is induction time's**.**

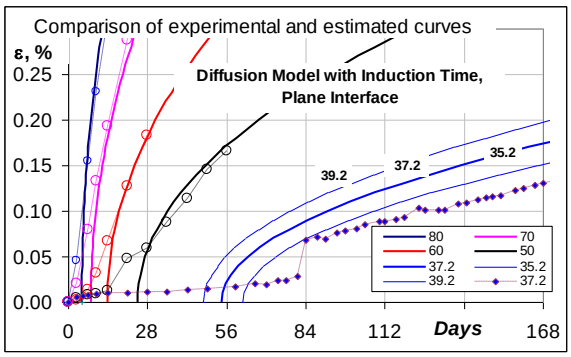

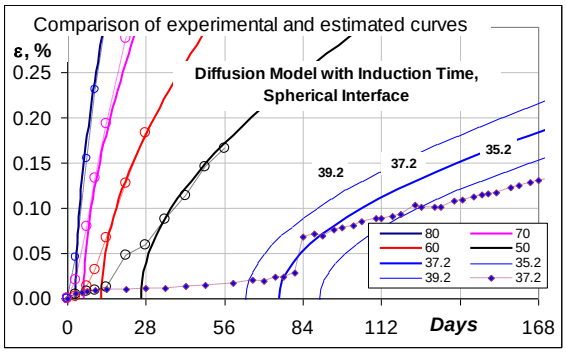

Figure 6 Comparison between estimated and experimental curves for models of diffusion with induction time, in the cases of plane (left) and spherical (right) interfaces, for points used in the fitting and independent run at 37.2ºC